Preprints of the 21st IFAC World Congress (Virtual)
Berlin, Germany, July 12-17, 2020

Hybrid Control Trajectory Optimization for Air-breathing Hypersonic Vehicle

Jaebong Song * **Han-lim Choi** **

* *Department of Aerospace Engineering, KAIST, Daejeon, Korea(e-mail: jbsong@lics.kaist.ac.kr)*
** *Department of Aerospace Engineering, KAIST, Daejeon, Korea(e-mail: hanlimc@kaist.ac.kr)*

Abstract: Trajectory optimization problem for air-breathing hypersonic vehicle is addressed in this paper. The engine of hypersonic vehicle is assumed as a dual-mode scramjet engine which can be operated as a ramjet and scramjet for wide range of flight Mach number. Boost-skipping trajectory was proposed for range maximization of hypersonic vehicle, and based on this trajectory, flight modes of dual-mode scramjet are divided into three modes, which are ram mode, scram mode, non-powered mode. Hypersonic vehicle was modelled with consideration of changes of physical quantities over mode transition. To deal with discrete mode changes as well as continuous control, hybrid optimal control method is applied to this problem. Simulation results demonstrate that the optimized trajectory with hybrid control has better performance compared to cyclic mode transition trajectory. Also, a vehicle which imitates the characteristics of dual-mode scramjet vehicle is implemented to optimize the trajectory. The results suggest that the hybrid optimal control can be applied to the trajectory optimization of a dual-mode scramjet vehicle considering the mode transition in infinite time horizon.

Keywords: Hypersonic vehicle, dual-mode scramjet, hybrid control, trajectory optimization, air-breathing engine

1. INTRODUCTION

In recent decades, interests on air-breathing hypersonic technologies have increased rapidly. Air-breathing propulsion system uses air in the atmosphere as an oxidizer, so there is no need to transport oxygen tanks. In addition, air-breathing supersonic and hypersonic engines have simpler structures than turbine engines. Research on the air-breathing hypersonic vehicles was focused primarily on weapon development at the first time. However, its simplicity, light-weight, high-speed, mission-flexibility, reusability and possibly long distance flight enable new possible approaches to intercontinental transport and orbital launch vehicles. Therefore, air-breathing hypersonic technologies are actively being studied in many countries.

The structure of air-breathing hypersonic vehicle is relatively simple, but the control problems of the integrated model are quite challenging. Therefore, studies on air-breathing hypersonic vehicle problems are largely classified into system modeling, nonlinear control with system characteristics, and trajectory optimization. The first attempt to an analytical model of longitudinal dynamics and control of air-breathing hypersonic vehicles was done by Chavez and Schmidt (1994). Newtonian impact theory was used to express the pressure distribution which is dependent on the Mach number, freestream pressure, angle of attack, and the vehicle geometry. After Chavez and Schmidt (1994), Michael A. Bolender studied the longitudinal dynamics of an air-breathing hypersonic vehicle with interactions between propulsion system, aerodynamics, and structure dynamics in Bolender and Doman (2005), Bolender and Doman (2007), and Bolender (2009).

Trajectory optimization using Gauss pseudospectral method was performed in Tawfiqur et al. (2012) as part of trajectory optimization for air-breathing hypersonic vehicles. In Tawfiqur et al. (2012), aerodynamics, specific impulse, and thrust are formed as functions of Mach number and angle of attack which are curve-fitted using experimental data. The flight phase is divided into a boost-ascent trajectory and a cruise-dive trajectory, and optimization is performed as a multi-phase optimization problem. In Prasanna et al. (2005), trajectory optimization for cruising of air-breathing hypersonic vehicle was studied. The specific impulse for an air-breathing hypersonic vehicle was expressed as a function of Mach number and altitude by spline interpolation. And the trajectory was divided into ascending and cruising phase, and nonlinear programming method was used for optimization. In Tawfiqur et al. (2012) and Prasanna et al. (2005), one of the goal of the optimization problem is maximizing the range. Both studies have attempted to maximize the range with continuous engine combustion. However, as in Carter et al. (1998) and Li and Shi (2012), periodic hypersonic cruise trajectories effectuate better fuel-consumption savings during the same distance flight over steady-state cruise trajectories. Thus, the periodic cruise trajectory has longer range than the steady-state cruise trajectory using the same amount of fuel. The periodic cruise trajectory is divided into boost, periodic cruise, glide and landing phases. In the boost phase, the vehicle is accelerated by an auxiliary engine,

such as a rocket, because the high speed is required to turn on the air-breathing hypersonic engine. During the periodic cruise phase, the vehicle performs the skipping flight by periodically turning the engine on and off. The glide and landing phase is the terminal flight phase with little impact on the entire flight range. In Chai et al. (2015), this skipping phase trajectory is optimized for air-breathing scramjet missile to maximize the range of skipping phase. The trajectory optimization problem was solved with the hp-adaptive Gauss pseudospectral method which produces fast convergence, and accurate solutions. The scramjet engine turns on and off via break cycle, and the resulted trajectory was compared with the trajectories of normal cycle, and continuous cruise mode. As a result, the scramjet missile with break cycle has the longest trajectory among others. However, rather than turning on and off the engine in a cyclic manner, it is expected to yield longer range of the vehicle if switching on and off is decided optimally. Thus, in this paper, hybrid control trajectory optimization for range maximization of an air-breathing hypersonic vehicle is introduced. Moreover, the dual-mode scramjet engine model is used to cover a wide range of flight Mach number.

The ramjet and scramjet engines are well-known supersonic and hypersonic engine models. The difference between those engines is the speed of airflow in the combustor. For ramjet, airflow is compressed and decelerated to subsonic speed in inlet. And this subsonic flow is mixed with fuel in combustor. For scramjet, airflow is also compressed and decelerated in inlet, but still kept in supersonic speed. Therefore, combustion is occurred in supersonic speed. Because ramjet compresses airflow to subsonic speed, it causes massive loss of total pressure which is related to thrust, thus ramjet engine is known as more efficient in Mach 3 to 5, and scramjet is for over Mach 5. There are separate favorable flight speed regions for ramjet and scramjet engines, therefore, the dual-mode scramjet vehicle concept which combines ramjet and scramjet engine has been proposed to cover the wide range of flight speed regions. Thus the dual-mode scramjet vehicle requires transitions between ram and scram mode during its flight. The ram-scram transition for dual-mode scramjet vehicles by the flight conditions and control inputs was studied in Dalle and Driscoll (2013). Although subsonic combustion of ramjet and supersonic combustion of scramjet can occur in same flow path, the steady-state thrust is discontinuous over mode transition. Also, Fotia (2014) demonstrated the discontinuous characteristics of mode transition between ram and scram mode. Non-allowable flow configurations are identified through the transitions which means the discontinuities of thrust, entropy, and pressure recovery over mode transition are inevitable.

Due to discontinuous changes of physical quantities, such as thrust, over the transitions, ram and scram modes have to be considered as separate modes. Therefore, to deal with flight trajectory optimization for dual-mode hypersonic vehicles, the optimization problem has to solve the discrete decision changes between ram and scram modes over continuous flight control. In this paper, the hybrid optimal control has been applied to solve the trajectory optimization problem of air-breathing dual-mode hypersonic vehicle. Hybrid control problem is a combination of discrete and continuous control. And hp-adaptive Gauss pseudospectral method has been combined with hybrid optimal control problem to decide the optimal transition time between ram-mode, scram-mode and non-powered mode in infinite time horizon.

This paper is organized as follows. Section 2 gives problem formulations of trajectory optimization for the single-mode and the dual-mode hypersonic vehicle. At the first part of section 2, boost-skipping trajectory optimization for the single-mode scramjet vehicle, the hybrid optimal trajectory is compared with the periodic cruise trajectory which is presented in Chai et al. (2015). At the second part of section 2, the hybrid optimal trajectories are compared with varying the type of vehicles, such as ram-scram dual-mode, scram single-mode, and ram single-mode vehicle. In Section 3, formulation of hybrid optimal control problem is introduced. And simulation results and conclusions are presented in Section 4 and 5.

2. PROBLEM FORMULATION

The objective of optimization problems stated in this section is to maximize the range at the final time in the skipping phase. Therefore, the minimization problem is formulated as,

$$min \;\; J = -L_{t_f} \tag{1}$$

subjected to various constraints in the skipping phase.

2.1 Boost-skipping trajectory optimization for the single-mode scramjet vehicle

Boost-skipping trajectory for single-mode scramjet vehicle consists of a boost phase which accelerates by auxiliary power, such as a rocket booster, and skipping phase, which has scram modes and non-powered modes.

The nonlinear longitudinal equations of motion of the air-breathing hypersonic vehicle are described in Chai et al. (2015) as below

$$\begin{aligned}
\dot{L} &= \frac{Rv\cos\theta}{R+h} \\
\dot{h} &= v\sin\theta \\
\dot{v} &= \frac{1}{m}(T\cos\alpha - C_D qs) - g\sin\theta \\
\dot{\theta} &= \frac{1}{mv}(T\sin\alpha + C_L qs + F_N\cos\alpha) - (\frac{g}{v} - \frac{v}{R+h})\cos\theta \\
\dot{m} &= -\frac{T}{I_{sp}g} \\
n_y &= \frac{(T\sin\alpha + C_L qs + F_N\cos\alpha)}{mg}
\end{aligned} \tag{2}$$

where m is the mass of the vehicle, L is the downrange, h is the altitude, v is the flight velocity, α is the angle of attack, θ is the flight path angle, T is the thrust of scramjet and F_N is the thrust of lateral jets. n_y is the normal overload, q is dynamic pressure, s is the aerodynamic reference area of the vehicle, and R is the mean radius of the earth. C_D and C_L are aerodynamic drag and lift coefficients, which are the functions of angle of attack as below

$$C_L = 0.6203\alpha \tag{3}$$
$$C_D = 0.6450\alpha^2 + 0.0043378\alpha + 0.003772 \tag{4}$$

The specific impulse of the scramjet I_{sp} has a relationship with the flight Mach number, which is studied in Carter et al. (1998)

$$I_{sp}(Ma) = 7300\mathrm{e}^{-0.1599Ma} + 450 \tag{5}$$

The thrust T of scramjet is expressed as

$$\begin{aligned} T &= C_{t0} + C_{t1}\alpha + C_{t2}\alpha^2 + C_{t3}\alpha^3 \\ C_{t0} &= 6378.5\beta - 100.9 \\ C_{t1} &= 35542\beta - 2421.6 \\ C_{t2} &= 26814\beta - 12777 \\ C_{t3} &= -376930\beta - 37225 \end{aligned} \tag{6}$$

where β is the throttle coefficient of the scramjet. For simplicity, β can be considered as a constant value as $\beta = 0.8$. Therefore, the thrust of scramjet is only function of angle of attack. The control variables are $u = (\alpha, F_N)^T$.

Following trajectory constraints are considered in simulation:

(1) Angle of attack constraint

Angle of attack is constrained by operation condition of scramjet in skipping phase.

$$|\alpha(t)| \leq 10^\circ \tag{7}$$

(2) Altitude constraint

The vehicle should keep flight in the near space to reduce drag and avoid ground defense system.

$$25km \leq h \leq 80km \tag{8}$$

(3) Terminal constraint

For the last phase of flight, dive phase, the vehicle has to be ensure enough kinetic energy.

$$\begin{aligned} h_f &\geq 25km \\ v_f &\geq 1500m/s \end{aligned} \tag{9}$$

(4) Thrust constraint for lateral jets

$$F_N \leq F_{N_{max}} \tag{10}$$

2.2 Boost-skipping trajectory optimization for the dual-mode scramjet vehicle

In this section, trajectory optimization for the dual-mode scramjet vehicle is studied. To cover wider range of flight Mach number, flight modes are divided into three modes which are ram mode, scram mode, and non-powered mode. In the previous section, the dynamic models and constraints follow as described in Chai et al. (2015). However, despite the fact that the lateral jet generates a significantly huge thrust relative to the vehicle mass, the lateral jet dynamics have not been modelled in detail. Therefore, in this section, the lateral jet is omitted from the longitudinal equations of motion as below

$$\begin{aligned} \dot{L} &= \frac{Rv\cos\theta}{R+h} \\ \dot{h} &= v\sin\theta \\ \dot{v} &= \frac{1}{m}(T\cos\alpha - C_D qs) - g\sin\theta \\ \dot{\theta} &= \frac{1}{mv}(T\sin\alpha + C_L qs) - (\frac{g}{v} - \frac{v}{R+h})\cos\theta \\ \dot{m} &= -\frac{T}{I_{sp}g} \\ n_y &= \frac{(T\sin\alpha + C_L qs)}{mg} \end{aligned} \tag{11}$$

And the control variable is only the angle of attack.

The thrust models for ram and scram mode should be modelled differently. For sophisticated modeling, thrust models of dual-mode scramjet engine is required, but so far the control problems of integrated dual-mode scramjet vehicle have not been studied actively yet. Thus, in this section, a simplified engine model which can imitate the characteristics of dual-mode scramjet engine is modelled as below

Table 1. Simplified specifications of the air-breathing dual-mode scramjet vehicle

	Engine type	
	Ram	Scram
Thrust(N)	6500	5000
Min speed(m/s)	800	1700
Max speed(m/s)	1700	5000

The aerodynamics are assumed to be same as the former problem. The specific impulse I_{sp} for both scram and ram engines follows the same relationship with Mach number as the previous section,

$$I_{sp}(Ma) = 7300\mathrm{e}^{-0.1599Ma} + 450 \tag{12}$$

The trajectory constraints are considered as follows

(1) Angle of attack constraint

$$|\alpha(t)| \leq 10^\circ \tag{13}$$

(2) Altitude constraint

$$15km \leq h \leq 100km \tag{14}$$

(3) Terminal constraint

$$\begin{aligned} h_f &\geq 20km \\ v_f &\geq 1000m/s \end{aligned} \tag{15}$$

3. FORMULATION OF HYBRID OPTIMAL CONTROL PROBLEM

Hybrid optimal control problem is a combination of discrete and continuous control. The car control problem with continuous acceleration with discrete gears is also a sort of hybrid optimal control problem. Ram-scram transition can be dealt as a similar manner of changing gears of a car. There are several studies to deal with hybrid optimal control, such as linear quadratic regulator(LQR) solution, mixed integer non-linear programming(MINLP), Rapidly-exploring random trees(RRTs), and differential dynamic programming(DDP). Some of these approaches

are confronted with limitations which are related to the increasing of computational load to decide every discrete action at every time step which is exponentially growing with the length of time horizon. Especially, the vehicle range maximization problem which is dealt in this paper, is nonlinear and has free final time. To face with these issues, stochastic dynamics concept for DDP problems is used. There are some policies for hybrid control trajectory optimization problems, such as greedy discrete actions choice, interpolated discrete actions choice, and mixture of discrete actions. In this paper, mixture of discrete actions policy is used with hp-adaptive Gauss pseudospectral method to solve hybrid optimal control problem with free final time.

Using mixture of discrete actions for hybrid control was proposed by Pajarinen et al. (2017). This approach assigns a continuous pseudo-probability to each discrete action. During optimization, specialized cost function compels these stochastic discrete actions into deterministic discrete actions.

Modified control $\hat{u}$ is

$$\hat{u} = \begin{bmatrix} u \\ p_a \end{bmatrix} \tag{16}$$

where p_a contains the action probabilities. The dimension of the control increases by the number of discrete actions.

For hybrid controls, the dynamics model $f(x, u, a)$ depends on both continuous controls u and discrete actions a. The proposed dynamic model is represented as

$$\hat{f}(x, \hat{u}) = \sum_a p_a f(x, u, a) \tag{17}$$

Modified dynamics $\hat{f} = (x, u, p)$ act like expected dynamics of total system. Additionally, for hybrid control, the specialized cost function $c(x, u, a)$ has to be defined as

$$\hat{c} = \sum_a \phi(p_a) c(x, u, a) \tag{18}$$

where $\phi(\cdot)$ is a smoothing function to make the Hessian of the cost function positive-definite w.r.t. the linear parameters p_a. Pseudo-Huber smoothing function is used as

$$\phi(p) = \phi(p, 0.01), \quad \phi(p, k) = \sqrt{p^2 + k^2} - k \tag{19}$$

which is close to linear but has a positive second derivative.

Furthermore, equality and inequality constraints are added to optimization problem,

$$0 \leq p \leq 1, \quad \sum_a p_a = 1 \tag{20}$$

To drive stochastic discrete actions into deterministic discrete actions, a cost function is assigned explicitly which increases during optimization. Following smoothed piecewise cost function is added to the cost function

$$c_{ST}(x, u, p) = C_{ST} \sum_a \begin{cases} \phi(p_a) & \text{if } p_a < p_{th} \\ \phi(\dfrac{(1 - p_a)}{p_{th}/(1 - p_{th})}) & \text{if } p_a \geq p_{th} \end{cases} \tag{21}$$

where $p_{th} = 1/N_a$, which is the number of types of discrete actions, and C_{ST} is an adaptive constant. If adaptive constant C_{ST} is increased during optimization, it allows smoothly increasing determinicity of discrete actions and then finally deterministic actions are selected.

In this paper, hybrid optimal control is combined with hp-adaptive Gauss pseudospectral method to deal with free final time. As described in algorithm 1, C_{ST} gets 2 times bigger for every loop of Gauss pseudospectral method and c_{ST} is added to the objective function. Therefore, to minimize the new objective function J_{new}, c_{st} becomes zero by forcing p_a to be 0 or 1, which means deterministic action are taken during the entire control time.

Algorithm 1 Hybrid optimal control with hp-adaptive Gauss pseudospectral method

```
Boundary conditions set B
Objective function J ← −L_{t_f}
Randomly initialize the state vector X ← x_0
Compute optimized state vector X_s via hp-adaptive GPM with J, B, and X
X ← X_s
C_ST ← 1
J_new ← −L_{t_f} + c_ST
for i = 1, 2, ..., N do
    Compute optimized state vector X_s via hp-adaptive GPM with J_new, B, X, and C_ST
    X ← X_s
    C_ST ← C_ST × 2
end for
return J_new, X
```

4. SIMULATION RESULTS

4.1 Boost-skipping trajectory optimization for single-mode scramjet vehicle

First, to compare the simulation results of hybrid optimal mode transition trajectory of air-breathing vehicle with existing trajectory optimization results which is based on cyclic mode transition, the results in Chai et al. (2015) are implemented. Cyclic mode transition is a sort of rule-based mode transition. When the vehicle reaches at the specific conditions, it starts to ignite or turn off the engine. In Chai et al. (2015), scramjet ignites when it starts to climb and its velocity decreases to $1500m/s$, which is designated for minimum ignition speed. And it turns off the engine when the vehicle reaches at 40km altitude.

Simulation conditions for cyclic mode transition are given as

(1) Initial conditions

$$\begin{aligned} v_0 &= 2000m/s, \quad \theta_0 = 25^\circ, \\ h_0 &= 40km, \quad L_0 = 0km, \\ m_0 &= 671kg, \quad m_f = 548kg \end{aligned} \tag{22}$$

(2) Final conditions

$$v_f \geq 1500m/s, \quad h_f \geq 25km \tag{23}$$

(3) Path constraints

$$\begin{aligned} n_{y,max} &= 10, \quad q_{max} = 50kPa, \\ \dot{Q}_{max} &= 250kW/m^2, \quad F_{N_{max}} = 4000N \end{aligned} \tag{24}$$

(4) Scramjet ignition conditions

$$v \leq 1500m/s, \quad h \leq 40km, \quad \theta \geq 0^\circ \tag{25}$$

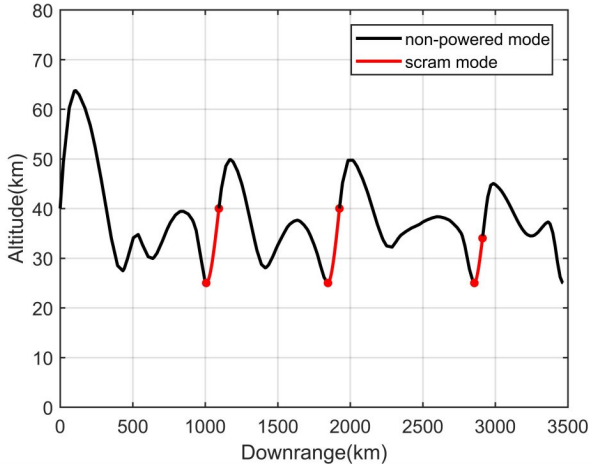

Fig. 1. Optimal trajectory of single-mode scramjet vehicle with cyclic mode transition. Red parts of trajectory depicts when the vehicle is in the scram mode, while black parts of trajectory is when the vehicle is in the non-powered mode.

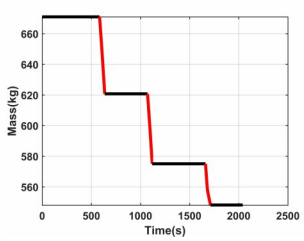

Fig. 2. Mass profile

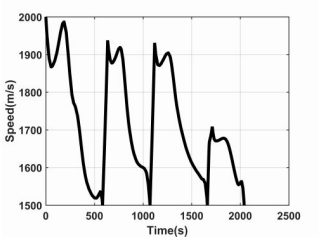

Fig. 3. Speed profile

Figure 1, 2 and 3 are implemented results of Chai et al. (2015). Figure 1 shows the overall optimal trajectory of scramjet vehicle with cyclic mode transitions. And the mass profile and speed profile of the vehicle is described in Figure 2 and 3, respectively. Total three times of scramjet ignition are occurred during the flight and six times of mode change accordingly. The terminal flight range is 3467km and the flight time is 2040s.

Subsequently, hybrid control trajectory optimization is simulated and Figure 4, 5 and 6 are results. In this case, scramjet ignition condition is differ from the former case. Ignitions can be occurred freely only if the speed of vehicle is larger than the minimum ignition speed which is 1500m/s, while there are certain rules on altitude, flight path angle and speed for cyclic mode transitions. Other conditions, such as initial and final conditions and path constraints, are same as Eq (22)–(24). Figure 4 shows the resulting optimal trajectory of single-mode scramjet vehicle with hybrid optimal control. The scramjet engine on/off points are optimally chosen for range maximization. And the consequent mass and speed profiles over the flight are presented in Figure 5 and 6. On every ignition starting point, the speed of vehicle is kept over the minimum ignition speed, 1500m/s. The terminal flight range is 4796km and the flight time is 2490s. Accordingly, hybrid optimal mode transition yields 1.38 times longer range and 1.22 times larger flight time than cyclic mode transition.

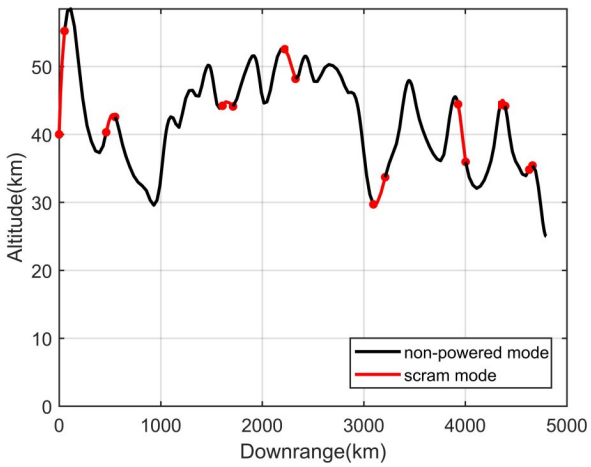

Fig. 4. Optimal trajectory of single-mode scramjet vehicle with hybrid optimal control. As described before, red parts of trajectory are in scram mode and black parts are in non-powered mode.

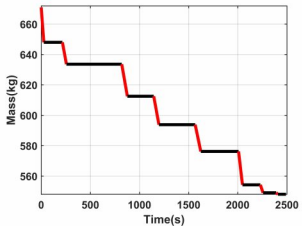

Fig. 5. Mass profile

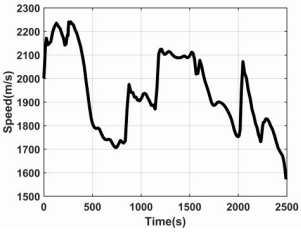

Fig. 6. Speed profile

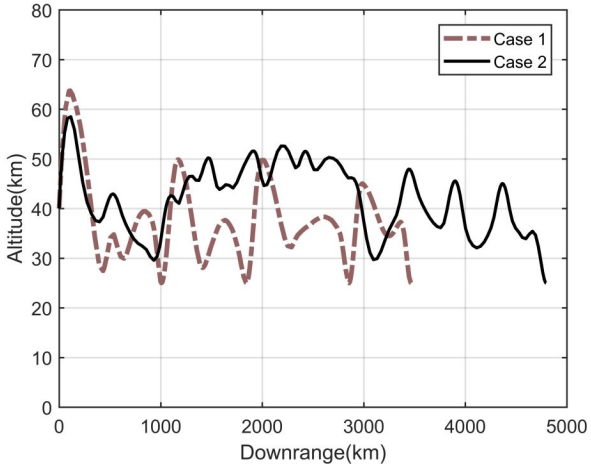

Fig. 7. Comparison of optimized trajectory between cyclic mode transition and hybrid optimal mode transition. Case 1, in dotted line, is the result of cyclic mode transition and Case 2, in solid line, is the result of hybrid optimal mode transition.

4.2 Boost-skipping trajectory optimization for dual-mode scramjet vehicle

In previous section, hybrid optimal trajectory of single-mode scramjet vehicle is compared with existing cyclic trajectory of single-mode scramjet vehicle and shows better performance in range maximization. Therefore, in this

Table 2. Comparison of range and flight time between two different mode transition policies

cyclic mode transition		hybrid optimal mode transition	
range(km)	flight time(s)	range(km)	flight time(s)
3467	2040	4796	2490

section, simulation results of hybrid optimal mode transition trajectory of dual-mode scramjet vehicle are presented with the results of hybrid optimal trajectory of each single-mode vehicle which are the single-mode ramjet vehicle and the single-mode scramjet vehicle. Minimum and maximum speed for igniting each of these engines are described in Table 1. Therefore, simulation conditions are given as

(1) Initial condition

$$\begin{aligned} v_0 &= 2000m/s, \quad \theta_0 = 25^\circ, \\ h_0 &= 40km, \quad L_0 = 0km, \\ m_0 &= 671kg, \quad m_f = 548kg \end{aligned} \tag{26}$$

(2) Final condition

$$v_f \geq 1000m/s, \quad h_f \geq 20km \tag{27}$$

(3) Path constraints

$$n_{y,max} = 10 \tag{28}$$

(4) Scram ignition condition

$$1700m/s \leq v \leq 5000m/s \tag{29}$$

(5) Ram ignition condition

$$800m/s \leq v \leq 1700m/s \tag{30}$$

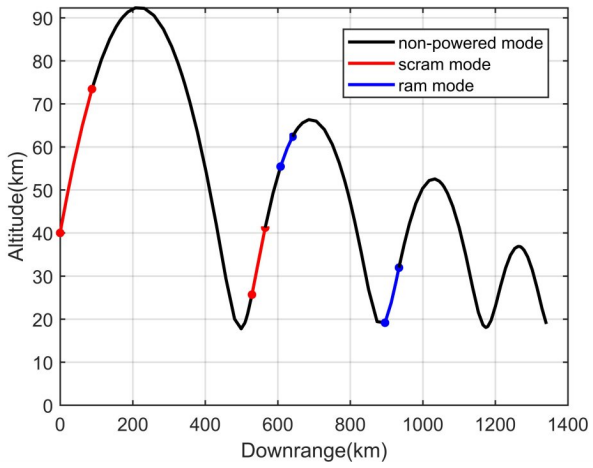

Fig. 8. Optimal trajectory of dual-mode hypersonic vehicle with hybrid optimal control. Red parts are trajectory in scram mode flight, blue parts are in ram mode flight, and the rests are non-powered mode.

Figure 8, 9 and 10 represents optimized trajectory, mass profile, and speed profile of ram-scram dual-mode vehicle, respectively. In Figure 8, the trajectory consists of two scram modes and two ram modes, and the rests are non-powered modes. Because the initial velocity exceeds 1700m/s, which is minimum ignition speed for scramjet engine, scram mode starts for the first 45 seconds. After speeding up during scram mode, the vehicle can skip about

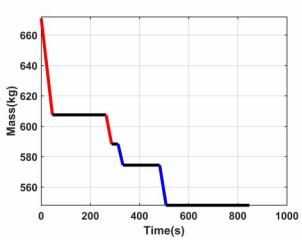

Fig. 9. Mass profile

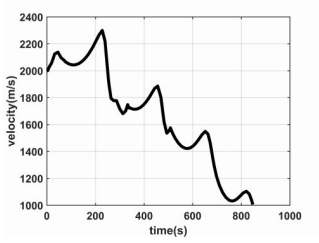

Fig. 10. Speed profile

a half band. And then, it enters scram mode again and acceleration has slightly increased. However, the vehicle is in climbing trajectory and the speed keeps decreasing under minimum ignition speed for scramjet. Therefore, scramjet engine cannot ignite no more, and starts the first ramjet mode. Based on the speed gained from this ram mode, the vehicle flies about a half of band. Afterwards, it enters the last ram mode, as well as the last powered mode, and skips about 421.7km with zero thrust. The terminal range is 1356km and the flight time is 847.3s.

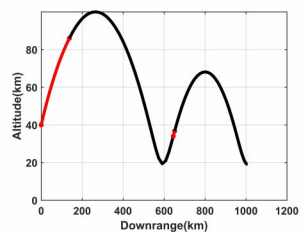

Fig. 11. Scram single-mode trajectory

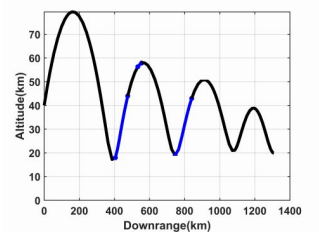

Fig. 12. Ram single-mode trajectory

Figure 11 and 12 shows the optimized trajectory of scram single-mode vehicle and ram single-mode vehicle with same conditions as Eq (26)–(30). In Figure 11, red parts of trajectory are in scram mode, and the rest parts are in non-powered mode. Similarly, in Figure 12, blue parts are in ram mode and the rest parts are in non-powered mode.

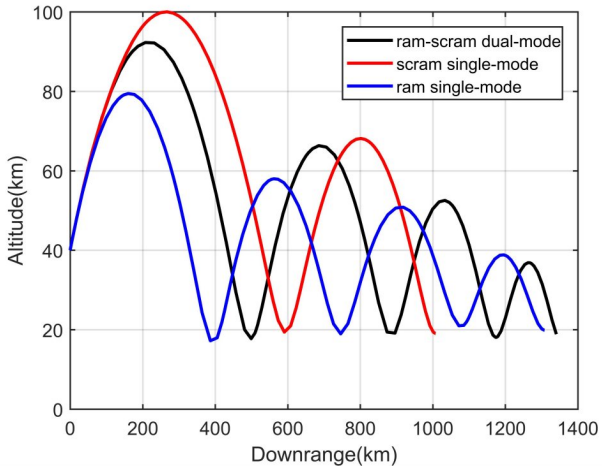

Fig. 13. Comparison of optimized trajectory between three different vehicles. Black line describes the ram-scram dual-mode vehicle, red line is for scram single-mode vehicle, and blue line is for ram single-mode vehicle.

The comparisons of dual-mode and two single-mode results are in Figure 13 to 15. The ram-scram dual-mode vehicle

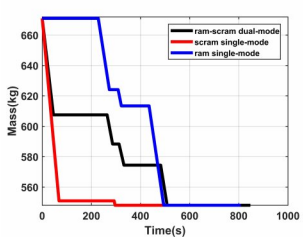

Fig. 14. Comparison of vehicle mass profile

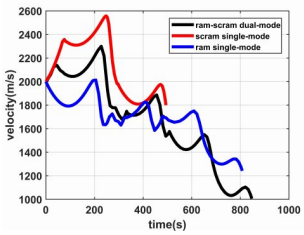

Fig. 15. Comparison of vehicle speed profile

has the longest range and flight time, which is 1356km and 847.3s. In the second place, ram single-mode vehicle has the terminal range of 1308km, and the flight time of 808s.

Table 3. Comparison of range and flight time between operational modes

	dual-mode	single-mode	
	ram-scram	scram	ram
range(km)	1356	1008	1308
flight time(s)	847.3	494.2	808
C_{ST}	128	128	512

5. CONCLUSIONS

This paper presents trajectory optimization for dual-mode hypersonic vehicle using hybrid optimal control with Gauss pseudospectral method. Based on boost-skipping trajectory, flight modes of the dual-mode scramjet vehicle are divided into three modes which are ram mode, scram mode, and non-powered mode. For the mode transitions over those separate modes with free final time, hybrid optimal control concept is applied. Simulation results show that hybrid optimal control has improved results on range maximization of single-mode scramjet vehicle over existing cyclic mode transition method. Afterwards, the hybrid optimal control is applied to the range maximization problem of a dual-mode scramjet vehicle and compared with scram and ram single-mode vehicle. And the results suggest that the hybrid optimal control with Gauss pseudospectral method can be used to the trajectory optimization problem of a dual-mode hypersonic vehicle considering the mode transition in infinite time horizon.

6. ACKNOWLEDGEMENT

This work was supported by Scramjet Combined Propulsion System Specialized Research Laboratory (No.16-106-501-035) of Korea.

REFERENCES

Bolender, M. and Doman, D. (2005). A non-linear model for the longitudinal dynamics of a hypersonic air-breathing vehicle. In *AIAA Guidance, Navigation, and Control Conference and Exhibit*, 6255.

Bolender, M.A. (2009). An overview on dynamics and controls modelling of hypersonic vehicles. In *American Control Conference, 2009. ACC'09.*, 2507–2512. IEEE.

Bolender, M.A. and Doman, D.B. (2007). Nonlinear longitudinal dynamical model of an air-breathing hypersonic vehicle. *Journal of spacecraft and rockets*, 44(2), 374–387.

Carter, P.H., Pines, D.J., and Rudd, L.V. (1998). Approximate performance of periodic hypersonic cruise trajectories for global reach. *Journal of aircraft*, 35(6), 857–867.

Chai, D., Fang, Y.W., Wu, Y.l., and Xu, S.h. (2015). Boost-skipping trajectory optimization for air-breathing hypersonic missile. *Aerospace Science and Technology*, 46, 506–513.

Chavez, F.R. and Schmidt, D.K. (1994). Analytical aeropropulsive-aeroelastic hypersonic-vehicle model with dynamic analysis. *Journal of Guidance, Control, and Dynamics*, 17(6), 1308–1319.

Dalle, D.J. and Driscoll, J.F. (2013). Flight mechanics of ram-scram transition. In *AIAA Atmospheric Flight Mechanics (AFM) Conference*, 4687.

Fotia, M.L. (2014). Mechanics of combustion mode transition in a direct-connect ramjet–scramjet experiment. *Journal of Propulsion and Power*, 31(1), 69–78.

Li, R. and Shi, Y. (2012). The fuel optimal control problem of a hypersonic aircraft with periodic cruising mode. *Mathematical and Computer Modelling*, 55(11-12), 2141–2150.

Pajarinen, J., Kyrki, V., Koval, M., Srinivasa, S., Peters, J., and Neumann, G. (2017). Hybrid control trajectory optimization under uncertainty. In *Intelligent Robots and Systems (IROS), 2017 IEEE/RSJ International Conference on*, 5694–5701. IEEE.

Prasanna, H., Ghose, D., Bhat, M., Bhattacharyya, C., and Umakant, J. (2005). Interpolation-aware trajectory optimization for a hypersonic vehicle using nonlinear programming. In *AIAA Guidance, Navigation, and Control Conference and Exhibit*, 6063.

Tawfiqur, R., Zhou, H., Sheng, Y.Z., Younis, Y.M., and Zhang, K.N. (2012). Trajectory optimization of hypersonic vehicle using gauss pseudospectral method. In *Applied Mechanics and Materials*, volume 110, 5232–5239. Trans Tech Publ.